

SCHOOL OF
CHEMICAL ENGINEERING



THE UNIVERSITY
of ADELAIDE

Supporting Information

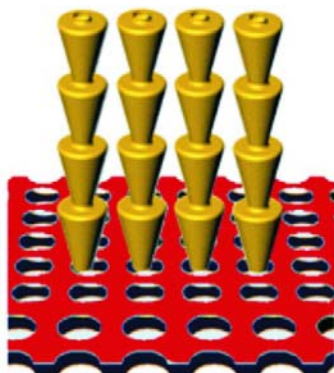
***In situ* monitored engineering of inverted nanoporous anodic alumina funnels: On the precise generation of 3D optical nanostructures**

Abel Santos*, Tushar Kumeria, Ye Wang and Dusan Losic*

School of Chemical Engineering, The University of Adelaide, SA 5005, Australia

*E-Mails: abel.santos@adelaide.edu.au / dusan.losic@adelaide.edu.au

Losic
Group



**NanoTech
Research**

S1. Linear Fittings for ΔOT_{eff} and d_p with Etching Time

To establish the dissolution rate of mono-stratified NAA within each of the etching stages, the pore diameter (d_p) was measured by SEM image analysis at equidistant points of the etching process (i.e. every 500 and 320 s for mono-stratified NAA produced in oxalic and sulphuric acids, respectively). This was used to establish a direct relationship between ΔOT_{eff} and d_{r-NAA} , which was obtained by applying linear fittings within each of the four different stages of the etching process (Fig. 1S).

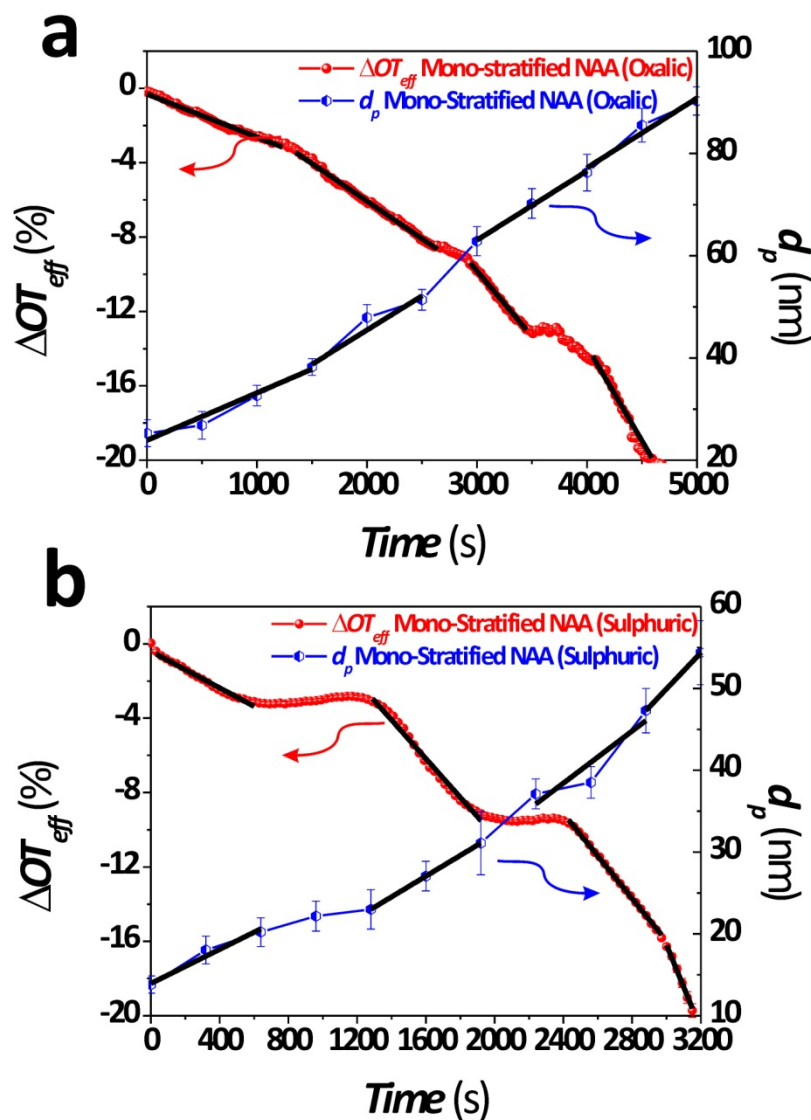


Fig. 1S. Linear fittings (black solid lines) used to establish the relationship between ΔOT_{eff} and d_p performed in H_3PO_4 5wt% at $35^\circ C$ flowed at $100 \mu L \text{ min}^{-1}$. a) Mono-stratified NAA produced in oxalic acid. b) Mono-stratified NAA produced in sulphuric acid.

S2. Effect of Annealing Temperature, Bath Temperature and Flow Rate on the Chemical Dissolution Rate of NAA

Fig. 2S summarises the effects of the annealing temperature, bath temperature and flow rate on the dissolution rate of NAA. As this figure shows, while d_{r-NAA} decreases with T_{an} , it increases with T_{bath} and v_f . The results reveal that those NAA samples produced in oxalic acid and thermally treated at 500 and 600°C (**Fig. 2Sa**) presented one and two additional shoulders, respectively. This phenomenon could be associated with the thermal decomposition of carboxylate impurities contained in the structure of NAA at temperatures above 400°C. This thermal decomposition of carboxylate impurities would result in the generation of additional chemical layers in the structure of NAA produced in oxalic acid.

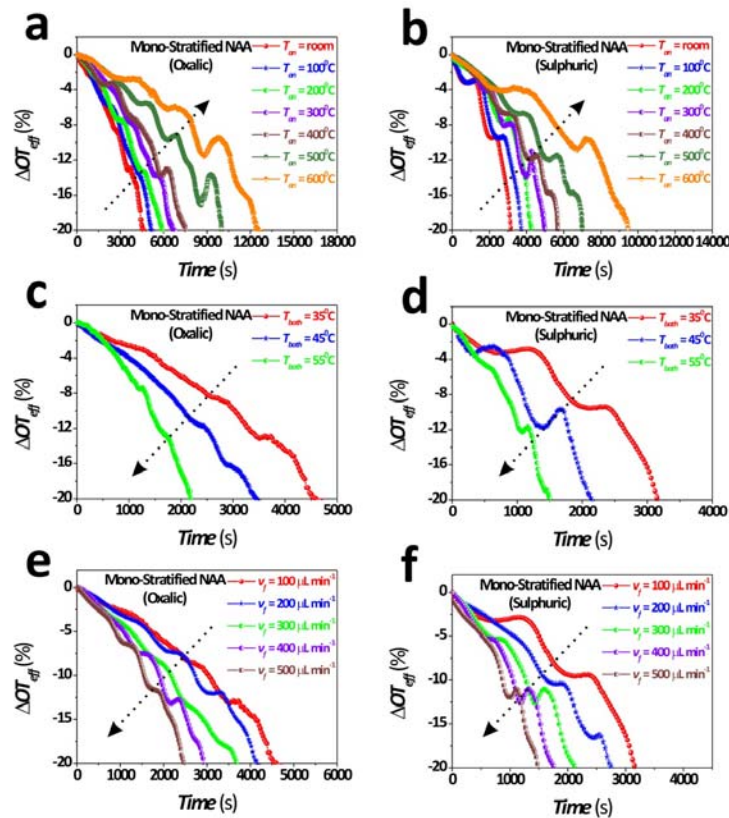


Fig. 2S. Effect of annealing temperature, bath temperature and flow rate on ΔOT_{eff} for mono-stratified NAA produced in oxalic and sulphuric acids. a-b) Evolution of ΔOT_{eff} with the etching time for mono-stratified NAA produced in oxalic and sulphuric acids at different annealing temperatures (from room to 600°C). c-d) Evolution of ΔOT_{eff} with the etching time for mono-stratified NAA produced in oxalic and sulphuric acids etched at different bath temperatures (from 35 to 55°C). e-f) Evolution of ΔOT_{eff} with the etching time for mono-stratified NAA produced in oxalic and sulphuric acids etched at different flow rates (from 100 to 500 $\mu\text{L min}^{-1}$).

S3. RfS Spectra of Mono-, Bi- and Tri-Stratified NAA

Fig. 3S shows RfS spectra of mono-stratified, bi-stratified and tri-stratified NAA produced in oxalic and sulphuric acids. The RfS spectrum of these NAA structures obtained at normal incidence displays a more complex pattern as the number of layers in the NAA structure increased from one to three. This results from the interference of light in all the layers of the Fabry–Pérot cavity based on NAA.

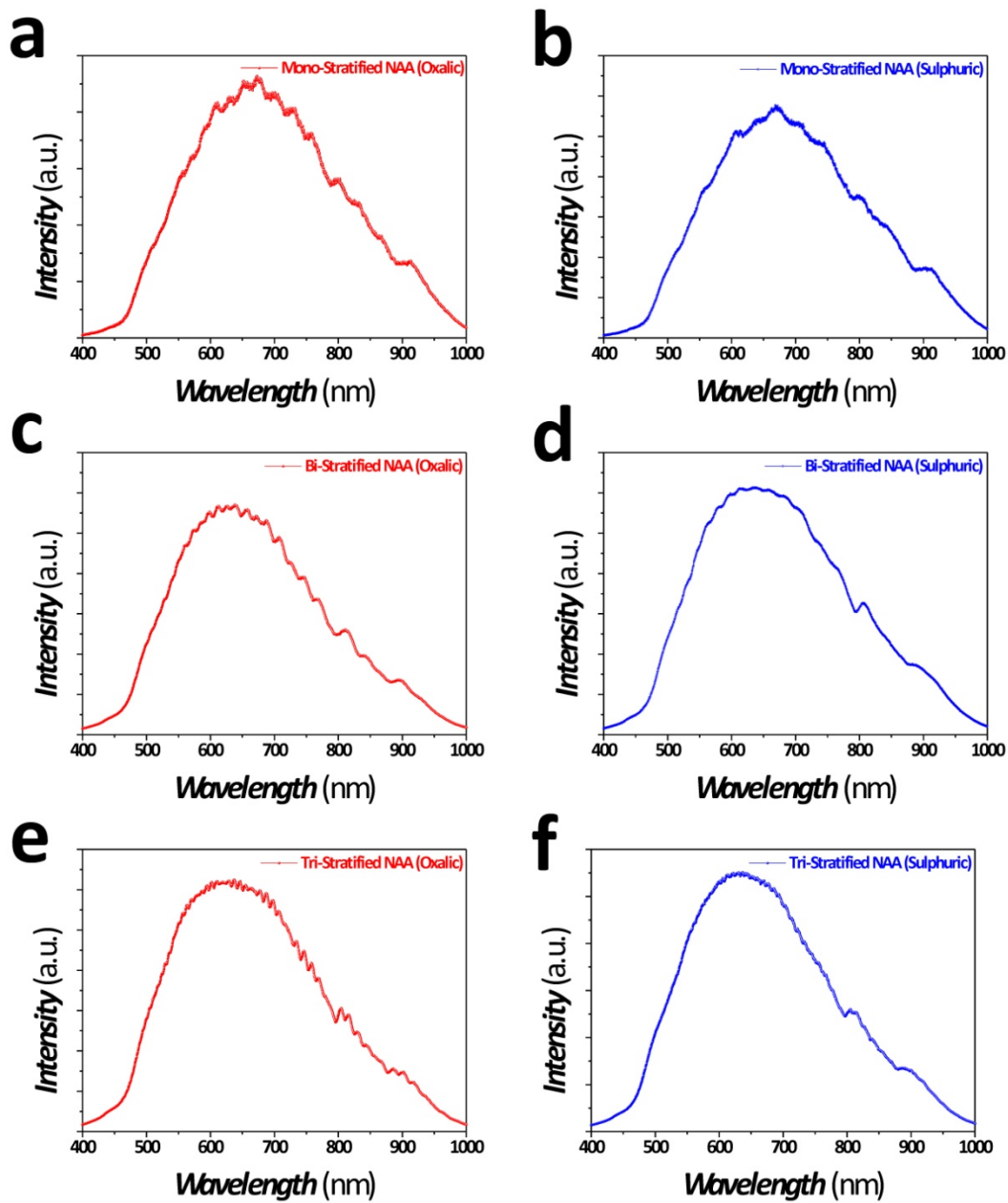


Fig. 3S. Examples of RfS spectra for mono-stratified, bi-stratified and tri-stratified NAA produced in oxalic (a, c and e) and sulphuric (b, d and f) acids.